science, engineering and health studies

Research Article

Science, Engineering and Health Studies
https://lio1.tci-thaijo.org/index.php/sehs
ISSN (Online): 2630-0087

Au-loaded TiO_2: A photocatalyst for photocatalytic hydrogen production with formic acid as a hole scavenger

Karnnapus Dangsakol[1], Cheewita Suwanchawalit[2], and Tarawipa Puangpetch[1]*

[1]Department of Chemical Engineering, Faculty of Engineering and Industrial Technology, Silpakorn University, Nakhon Pathom 73000, Thailand
[2]Department of Chemistry, Faculty of Science, Silpakorn University, Nakhon Pathom 73000, Thailand

***Corresponding author**: Tarawipa Puangpetch puangpetch_t@su.ac.th*

***Received**: 4 April 2024*
***Revised**: 24 September 2025*
***Accepted**: 5 October 2025*
***Published**: 19 December 2025*

***Citation**: Dangsakol, K., Suwanchawalit, C., & Puangpetch, T. (2025). Au-loaded TiO_2: A photocatalyst for photocatalytic hydrogen production with formic acid as a hole scavenger. Science, Engineering and Health Studies, 19, 25040012.*

ABSTRACT

Three methods successfully synthesized the TiO_2 photocatalysts: sol-gel, solvothermal, and flame spray pyrolysis. Au was loaded onto the synthesized TiO_2 photocatalysts via three methods: incipient impregnation, photo-deposition, and single-step doping. All synthesized TiO_2 photocatalysts were characterized by XRD, N_2 physisorption, TEM, UV-vis spectroscopy, H_2 chemisorption, and photoluminescence spectroscopy. The results pointed out that only sol-gel and solvothermal methods could provide the pure anatase-phase TiO_2. The anatase-phase, mesoporous-agglomeration structure of nano-crystallite size particles, suitable pore diameter, and relatively high surface area of the solvothermal-synthesized TiO_2 were the key properties that played important roles in maximizing its pristine-form photocatalytic activity in hydrogen production via photodegradation of formic acid under visible light irradiation. With Au loading by the photo-deposition method, the highest dispersion of Au on the TiO_2 surface and an acceptably low recombination rate of electron-hole pairs were achieved, yielding the most desirable Au-loaded, solvothermal-synthesized TiO_2 photocatalyst with the highest H_2 production rate of ~6,000 $\mu mol_{H2}/h/g_{cat}$.

Keywords: TiO_2; mesoporous assembly; photodegradation; hydrogen; clean energy

1. INTRODUCTION

Photocatalytic water splitting for H_2 production is an environmentally friendly reaction that utilizes clean and abundant solar energy to generate an electron-hole pair to conduct a degradation reaction. This technology not only can be used to produce clean and renewable fuel as H_2 (Sreethawong et al., 2008, 2009b; Sasikala et al., 2009; Puangpetch et al., 2010; Yan & Yang, 2011; Ahmad et al., 2020; Gupta et al., 2022), and eliminate pollutants (Kang et al., 2005; Gonzalez et al., 2008; Khtaee & Kasiri, 2010; Chiarello et al., 2010; Lin et al., 2012, Chung et al., 2023) separately, but also can be used to produce H_2 and eliminate pollutants simultaneously (Nam & Han, 2003; Patsoura et al., 2007; Puangpetch et al., 2011; Wang et al., 2023a; Yan et al., 2023; Guo et al., 2023). This research also focused on this valuable photocatalytic reaction. The previous research (Peng et al., 2008; Sreethawong et al., 2008; Puangpetch et al., 2008, 2009, 2011) pointed out that the mesoporous-assemble of the single-crystals structure is the important property that significantly enhances the photocatalytic activity of the photocatalyst. The meso-size of the pore matches the molecular size of water and provides better light-induced hydrophilicity. The aggregation of single crystals provides the high possibility of multi-electron transfer and the lower recombination between the photo-generated electrons and photo-generated holes. The disadvantage of aggregation is that it reduces the surface area of the photocatalyst. So, the present research aimed to find out the synthesis method that provided the

mesoporous-assembled TiO_2 photocatalyst with a high specific surface area. Three potential methods: sol-gel (Sreethawong et al., 2008; Puangpetch et al., 2008; Lee et al., 2010; Sadek et al., 2023; Solanki et al., 2022), solvothermal synthesis (Kang et al., 2001, 2005; Kang, 2003; Payakgul et al., 2005; Kongsuebchart et al., 2006; Khan et al., 2008; Cao et al., 2020; Wang et al., 2023b), and flame spray pyrolysis (Mueller et al., 2003; Strobel et al., 2006; Strobel & Pratsinis, 2007; Chiarello et al., 2008, 2010; Teoh et al., 2010; Boningari et al., 2018), and three Au modified methods: incipient impregnation, photodeposition, and single-step doping-were investigated in this study (Chan & Barteau, 2005; Pawinrat et al., 2009; Liu et al., 2010; Osterloh & Parkinson, 2011; Huang & Wey, 2011; Bouhadoun et al., 2015; Rodríguez-Martínez et al., 2020, Bhuskute et al., 2022). The photocatalytic activity in hydrogen production simultaneously with pollutant degradation of the synthesized Au-loaded TiO_2 photocatalysts was investigated via the photodegradation of formic acid as a model organic contaminant in wastewater from the natural rubber industry. The photodegradation of formic acid can be provided the different species formation, and the dominant pathways in hydrogen evaluation are as follows (Wang et al., 2002; Araña et al., 2004; Farias et al., 2009; Zhang & Zhang, 2009; Abdelli et al., 2023; Hayat et al., 2024):

$$CHOOH + H_2O \rightarrow HCOO^- + H^+$$

$$TiO_2 \xrightarrow{h\nu} e^- (\text{at } Ti^{+3d} \text{ site}) + h^+ (at\ O^{-2p} site)$$

At Ti^{+3d} site

$$CHOOH + e^- \rightarrow HCOO^- + H^+$$

$$2H^+ + 2e^- \rightarrow H_2$$

At Au site

$$CHOOH + e^- \rightarrow HCOO^- + H^+$$

$$2H^+ + 2e^- \rightarrow H_2$$

At O^{-2P} site

$$CHOOH + 2h^+ \rightarrow CO_2 + 2H^+$$

$$CHOO^- + h^+ \rightarrow CO_2 + \dot{H}$$

$$H_2O + h^+ \rightarrow \dot{O}H + H^+$$

2. MATERIALS AND METHODS

2.1 Materials

Tetraisopropyl orthotitanate (TIPT, Merck Co., Ltd., Bangkok, Thailand) was used as a titanium precursor. Acetylacetone (ACA, Merck Co., Ltd., Bangkok, Thailand) was used as a modifying agent for the TIPT in sol-gel synthesis. Distilled water, methanol (Avantor, Inc. (J.T. Baker), Bangkok, Thailand), ethanol (Avantor, Inc. (J.T. Baker), Bangkok, Thailand), 1,4-butanediol (Sigma-Aldrich Inc., Bangkok, Thailand), and xylene (K N Science Innovation Co., Ltd., Nonthaburi, Thailand) were used as solvents. Hydrogen tetrachloroaurate (III) trihydrate ($HAuCl_4 \cdot 3H_2O$, Sigma-Aldrich Inc., Bangkok, Thailand) was used as a gold precursor. Formic acid (Ajax Finechem Pty Ltd., Australia, by SNP Scientific Co., Ltd., Bangkok, Thailand) was used as a sacrificial reagent for photocatalytic H_2 production and simultaneously as a wastewater pollutant to be degraded. Commercial TiO_2 (P-25) (J.J. Degussa Hüls Co., Ltd., with 74% anatase phase and 26% rutile phase) was also used for comparative study.

2.2 Synthesis methods of TiO_2 photocatalysts

Sol-gel method (SG): An equimolar ratio of ACA with Ti was first introduced into TIPT, and then the mixed solution was cooled to room temperature. This mixed solution was added to the $EtOH_{(aq)}$ and continuously stirred to obtain a clear yellow solution. It was kept at 80°C for 1 day to conduct gel formation. The gel was dried at 80°C for 2 days. The dried gel was calcined at 500°C for 4 h under air flow condition (at 30 cm^3/min) with the 10°C/min heating rate to get TiO_2 photocatalyst.

Solvothermal synthesis method (ST): TIPT was dissolved in 1,4-butanediol in a tube chamber. The chamber was then placed in an autoclave. The gap between the chamber and the autoclave wall was filled with 1,4-butanediol. The headspace of an autoclave was purged by nitrogen to eliminate air before heating this reactor. The reactor was heated to 300°C (a heating rate of 2.5°C/min) and kept for 2 h. During the solvothermal reaction, it was continuously rotated at 300 rpm. After the cooldown period, the solid powder in the liquid phase was separated and then washed three times with methanol. The powder was calcined at 500°C for 4 h under air flow condition (at 30 cm^3/min) with the 10°C/min heating rate to get TiO_2 photocatalyst.

Flame spray pyrolysis method (FSP): TIPT was dissolved in xylene and then injected into the center of a methane/oxygen flame by a syringe pump with a volumetric flow rate of 5 ml/min while sprayed through a nozzle with the aid of oxygen to induce fine droplets. The pressure drop at a capillary tip was kept at 1.5 atm. The generated TiO_2 powder was collected via a glass-microfiber filter with the aid of a vacuum pump.

2.3 Methods of Au loading

Incipient impregnation (IMP): An appropriate amount of $HAuCl_4 \cdot 3H_2O$ was dissolved in distilled water to obtain an Au precursor solution. Each of all TiO_2 powders was then impregnated with the Au precursor solution to achieve a desired nominal Au loading of 0.26 wt.%. The Au-impregnated TiO_2 was kept at room temperature for 6 h before being dried at 110°C overnight. Then it was reduced at 200°C for 4 h by H_2 gas to obtain the Au-loaded TiO_2 photocatalyst.

Photodeposition (PD): An appropriate amount of $HAuCl_4 \cdot 3H_2O$ for a desired nominal Au loading of 0.5 wt.% was dissolved in 0.5 vol.% methanol aqueous solution to obtain an Au precursor solution. Each of all TiO_2 powders was then suspended in the Au precursor solution under UV irradiation (Hg lamp, TUV 11 W PL-S, Phillip) for 10 min. The Au-loaded TiO_2 by photodeposition powder was dried at 110°C for 12 h to obtain the Au-loaded TiO_2 photocatalyst.

Single-step doping (DP): An appropriate amount of $HAuCl_4 \cdot 3H_2O$ for a desired nominal Au loading of 0.26 wt.% was added directly into each Ti precursor solution of each synthesis method. The remaining steps were the same as their original synthesis procedures. The final products were the Au-loaded TiO_2 photocatalysts.

2.4 Photocatalyst characterizations

Crystallinity, purity, and crystallite structure of both pristine and all Au-loaded TiO_2 photocatalysts were analyzed by using X-ray diffraction (XRD, Siemens D5000) with a rotating anode generating monochromatic CuK_α radiation with a Ni filter. The operating conditions were 30

kV and 15 mA with a continuous scanning rate of 2°/min. Specific surface area, pore size distribution, and average pore size of all TiO_2 photocatalysts were analyzed by N_2 absorption–desorption using the BET BELSORP Π analyzer. The specific surface area was determined by the BET multipoint method, whereas the pore size distribution and average pore size were determined by the BJH method. The morphology of all TiO_2 photocatalysts and their particle sizes were examined by a transmission electron microscope (TEM, JEOL 2000 CX). The quantity of the loaded Au contained in the Au-loaded TiO_2 photocatalyst was determined by the inductively coupled plasma (ICP) technique. H_2 chemisorption was used to determine the approximately percentage of Au dispersion on the surface of TiO_2 photocatalyst (Meyer et al., 2004; Guzmán et al., 2009; Rusinque et al., 2019; Mahdavi-Shakib et al., 2021). The resulting number of Au particles was used to infer the dispersion of Au on a surface. Light absorption abilities of all TiO_2 photocatalysts were investigated by a UV-vis spectrophotometer with $BaSO_4$ as a reference. Photoluminescence (PL) spectroscopy was used to evaluate the recombination rate between the photo-generated electrons and holes.

2.5 Photocatalytic hydrogen production with formic acid as a hole scavenger

Photocatalytic H_2 production activities of the pristine and Au-loaded TiO_2 photocatalysts were investigated via formic acid photodegradation by considering a steady-state H_2 production rate at 3-h irradiation time as an indicator. The reaction was performed in a semi-batch, Pyrex glass reactor with an outer irradiating light source and an inner cooling water system. The volume of the reactor was 750-cm^3. The 16 fluorescent lamps (11 W PL-S 2P, Phillip) were used as a visible light source with a total irradiance of ~90 W/m^2. The light spectrum of this lamp consists of ~97% visible light and ~3% UV light. For all experiments, 0.025 g of the pristine or Au-loaded TiO_2 photocatalyst was suspended in 250 cm^3 of 0.1 M formic acid aqueous solution with the aid of a magnetic stirrer. Before starting the reaction, the reactor was kept in the dark and simultaneously deaerated by Ar gas bubbling for 20 min. After the deaerated step, the Ar flow rate was adjusted to 30 cm^3/min and then the reaction was started by irradiating with visible light for 5 h. The reaction temperature was kept at 30°C by using the internal cooling water system. The gas sample in the headspace of the reactor was analyzed for its hydrogen, oxygen, carbon dioxide, and carbon monoxide composition by an online gas chromatograph equipped with a thermal conductivity detector.

3. RESULTS AND DISCUSSION

3.1 Characterization results: Effects of synthesis methods

The TiO_2 photocatalysts were successfully synthesized by sol–gel, solvothermal, and flame spray pyrolysis methods. The XRD patterns of all TiO_2 photocatalysts synthesized by those three methods are shown in Figure 1a). TiO_2 photocatalysts synthesized by SG and ST methods show only the dominant peaks of (101), (103), (200), (105), (213), (116), and (107) planes of anatase TiO_2, revealing these two methods (SG and ST) provide the pure anatase–phase TiO_2 powder. The case of TiO_2 synthesized by the FSP method showed an additional low intensity peak at 2θ of about 27.5, which corresponds to the indices of the (110) plane of rutile TiO_2 (Puangpetch et al., 2011), revealing it exhibits both anatase and rutile phases. However, TiO_2 synthesized by FSP contained only approximately 5% rutile phase.

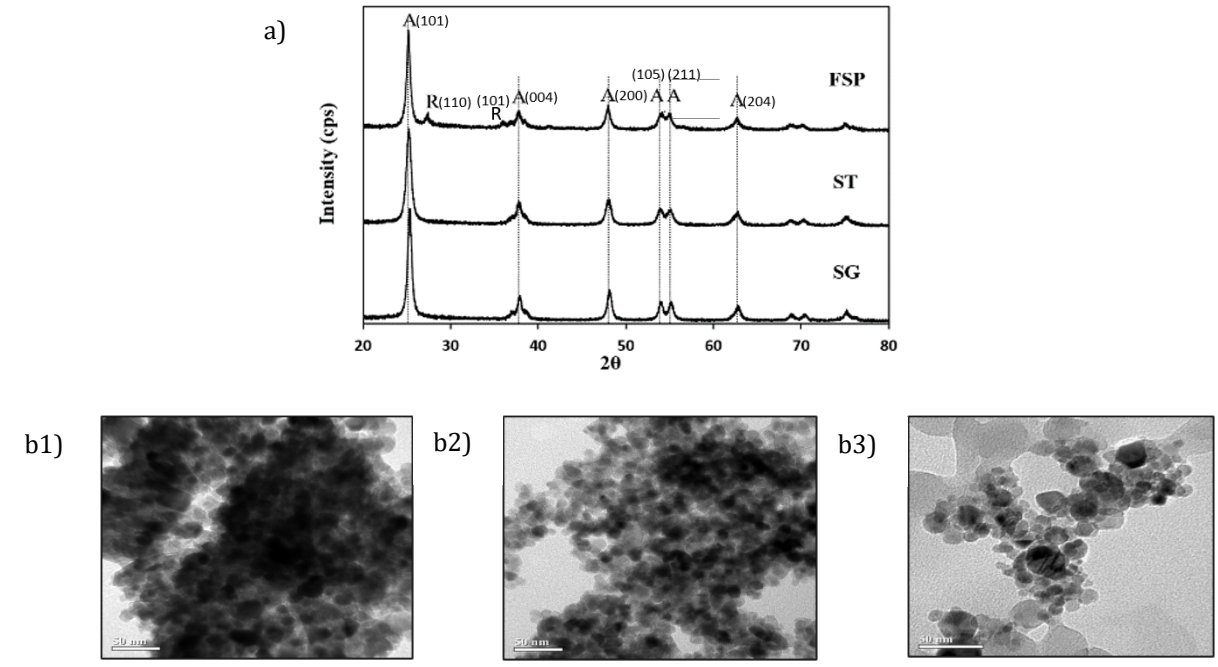

Figure 1. a) XRD patterns of the synthesized TiO_2 photocatalysts prepared by sol–gel method (SG), solvothermal synthesis method (ST), and flame spray pyrolysis (FSP) (A: anatase, R: rutile), b) TEM image of the synthesized TiO_2 preparation by b1) SG, b2) ST, and b3) FSP methods

The TEM was used to analyze the particle size and morphology of the synthesized TiO_2. The results are shown in Figure 1b and Table 1. The TEM results indicated that TiO_2 synthesized by all methods were spherical particles. The average particle size from the TEM image of each TiO_2 was similar to its crystallite sizes calculated from XRD results using the Scherrer equation (as shown in Table 1), indicating that a particle observed by TEM is a single crystal particle. The physical properties of all synthesized TiO_2 photocatalysts and the commercial TiO_2 (P25) are shown in Table 1. The results showed that the crystallite sizes of TiO_2 photocatalysts synthesized by three methods increased in the order of ST < SG < FSP. In addition, the crystallinity of the TiO_2 photocatalysts synthesized by the SG method exhibited higher crystallinity than that of those prepared by the ST and FSP methods. Both TiO_2 photocatalysts synthesized by ST and FSP showed similar crystallinity.

Table 1. Physical properties of the synthesized TiO_2 photocatalysts prepared by sol-gel method (SG), solvothermal synthesis method (ST), and flame spray pyrolysis (FSP)

Preparation method	Phase[a] content (% w/w)	d_{XRD}[b] (nm)	d_{TEM}[c] (nm)	Relative crystallinity[d]	S_{BET}[e] (m^2/g)	S_{XRD}[f] (m^2/g)	S_{BET}/S_{XRD}	Pore[e] diameter (nm)	Pore[e] volume (cm^3/g)
SG	A (100)	14.4	14.8	1.32	21.8	109.1	0.20	3.8	0.0591
ST	A (100)	11.8	12.1	1.00*	89.3	94.3	0.95	21.7	0.3716
FSP	A (86.8)	16.4	17.1	1.00	116.9	132.8	0.88	11.8	0.3856
	R (13.2)	17.0							
P25	-	-	-	-	61.8	-	-	28.0	0.3626

a) Calculated by the equation that was proposed by Payakgul et al. (2005)
b) Calculated by line broadening of XRD patterns
c) Determined from TEM images
d) The ratio between the height of the main peak of anatase patterns by using that of ST as reference
e) Calculated by the BET multipoint method
f) Surface area which the particles are assumed to be nonporous spheres ($S = 6/\rho d_{XRD}$)

Table 1 also shows the comparison results between the surface areas (S_{BET}) determined by the BET multipoint method and the surface area in which the particles are assumed to be nonporous spheres. It is discovered that S_{BET} is usually smaller than S_{XRD} due to the agglomeration of the single crystals (Payakgul et al., 2005). The BET surface area of the synthesized TiO_2 samples followed the order SG < ST < FSP. This suggested that the degree of agglomeration increased in the opposite order: FSP < ST < SG. The TEM results supported this conclusion (Figure 1–3b). In addition, TiO_2 synthesized by the SG method exhibited a highly agglomerated structure, leading to a significant internal surface area that may be inaccessible to nitrogen molecules during BET measurements. This could result in a discrepancy between the BET surface area (S_{BET}) and the XRD-based surface area (S_{XRD}), which was calculated assuming spherical crystallites with a uniform size distribution. TiO_2 synthesized by the ST method generally exhibited a less agglomerated structure compared to SG-synthesized TiO_2, resulting in a smaller discrepancy between its S_{BET} and S_{XRD} values. However, the S_{XRD} of ST-synthesized TiO2 remained slightly higher than the S_{BET}. In contrast, TiO_2 synthesized by the FSP method exhibited a highly dispersed structure with a large external surface area, leading to a negligible difference between S_{BET} and S_{XRD}.

Figure 2a) shows N_2 adsorption-desorption isotherms of the TiO_2 synthesized by SG, ST and FSP methods. The isotherms of TiO_2 synthesized by SG and ST exhibited the hysteresis loop and appear like the IUPAC type IV pattern, indicating the mesoporous structure (Rouquerol et al., 1999). However, the hysteresis loop in the isotherm of TiO_2 synthesized by the ST method shifted to higher partial pressure than that synthesized by the SG method. This is because TiO_2 synthesized by the ST method exhibited a larger pore size as compared to the TiO_2 synthesized by the SG method as shown in Figure 2b. The isotherm of TiO_2 synthesized by the FSP method is the IUPAC type II pattern (Rouquerol et al., 1999). TiO_2 synthesized by the FSP method was the non-mesoporous structure. Its pore size distribution was broad, and most part existed in the macroporous region (pore diameter >50 nm). The microporous characteristic was a typical property of nanoparticles obtained by the FSP method (Mueller et al., 2003; Strobel et al., 2006; Strobel & Pratsinis, 2007; Chiarello et al., 2008, 2010; Teoh et al., 2005). The total pore volume of the synthesized TiO_2 photocatalysts is showed in Table 1. TiO_2 synthesized by the SG method showed the lowest pore volume due to the agglomeration effect.

3.2 Characterization results: Effects of Au loading methods

The XRD patterns of Au-loaded TiO_2 prepared by photodeposition (PD), impregnation (IMP), and simultaneous doping (DP) are shown in Figure 3. All TiO_2-based photocatalysts were prepared by the ST method with the following condition: BD as a solvent, reaction temperature of 300°C, and calcination temperature of 500°C for 4 h. All XRD patterns exhibited only the on set peaks of the anatase phase, and the patterns were similar to that of the unmodified TiO_2 prepared by the ST method. No diffraction peak of Au at 2θ of about 44.0 (Hidalgo et al., 2009) in all XRD patterns implied that the loaded Au particles may be below 5 nm in diameter, which is the minimum size of the detected limitation of the XRD technique (Sreethawong et al., 2009a), and very high dispersion.

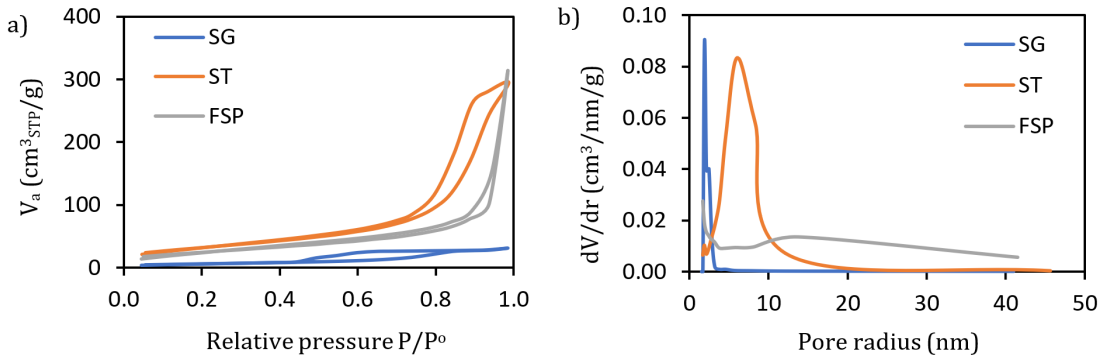

Figure 2. a) N_2 adsorption/desorption isotherms of TiO_2 synthesized by SG, ST and FSP methods, and b) pore size distributions of TiO_2 synthesized by SG, ST, and FSP methods

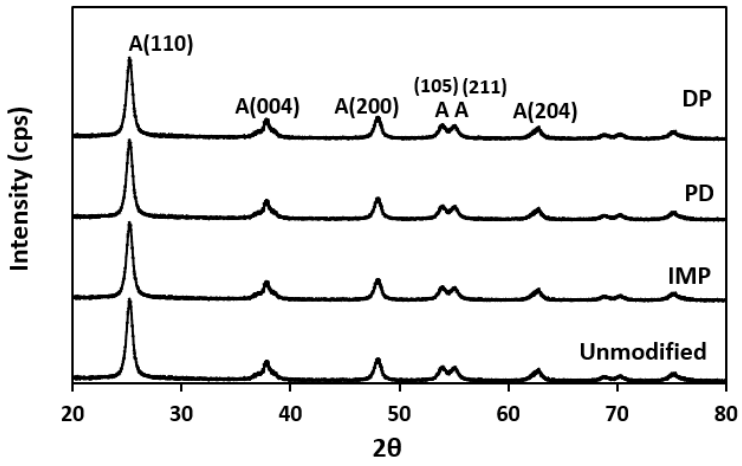

Figure 3. XRD patterns of the Au-loaded TiO_2 preparation by DP, PD, and IMP methods and the unmodified TiO_2

Moreover, three loading methods did not change the physical properties of the TiO_2-based photocatalysts from that of the unmodified TiO_2 as shown in Table 2 and Figure 4. All actual loadings of the Au-loaded on TiO_2 obtained from ICP analysis were not significantly different from the nominal Au loadings in the case of DP and IMP loading methods. However, the PD method provided the inequality of the actual loadings of the Au as compared to the nominal Au loading, as shown in Table 2. It could be concluded that the IMP and DP methods are suitable for the Au loading method and more reliably effective in amount control than the PD method.

H_2 chemisorption results of all the Au-loaded TiO_2 are also shown in Table 2. The Au-loaded TiO_2 by PD and DP methods exhibited higher Au dispersion than of by the IMP method. These results indicated that the Au active sites on the surface of the Au-loaded TiO_2 by PD and DP methods were higher than that of the Au-loaded TiO_2 by the IMP method.

Table 2. Physical properties of Au-loaded TiO_2 by IMP, PD, and DP

Au modified method	Actual Au loading[a] (% w/w)	d_{XRD}[b] (nm)	S_{BET}[c] (m^2/g)	Pore[c] diameter (nm)	E_g[d] (eV)	H_2 Chemisorption[e] (µmol/g)	Au Dispersion[e] (%)
Unmodified	-	11.8	116.9	11.8	3.26	n.d.	-
PD	0.26	11.7	101.2	11.3	3.18	12.1	36.67
IMP	0.25	11.7	112.5	12.2	3.10	7.9	24.9
DP	0.26	12.1	115.2	12.1	3.10	10.8	32.73

n.d. = not detected
a) ICP analysis (nominal loading = 0.5, 0.26, 0.26 wt.% for PD, IMP, and DP, respectively)
b) Calculated by line broadening of XRD patterns
c) Calculated by the BET multipoint method
d) UV-visible spectroscopy analysis
e) H_2 chemisorption analysis

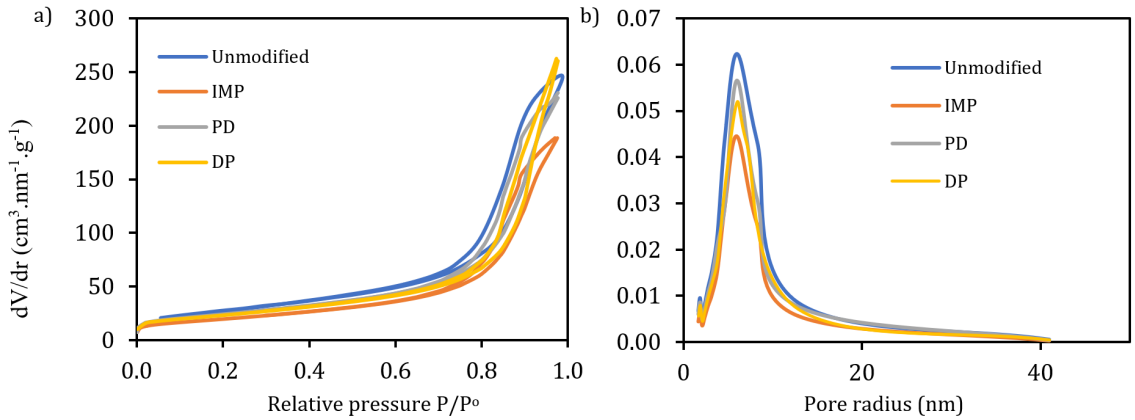

Figure 4. a) N_2 adsorption/desorption isotherms and b) Pore size distribution of Au-loaded TiO_2 by IMP, PD, and DP methods

The light-harvesting ability of all Au-loaded TiO_2 by IMP, PD, and DP methods was analyzed from their UV-vis: DRS graphs in the wavelength range from 200 to 800 nm as shown in Figure 5a. In the UV range spectra, the absorptions were very similar for all Au-loaded TiO_2. The characteristic absorption threshold was around 400 nm and close to that of unmodified TiO_2. The band gap energy of all Au-loaded TiO_2 photocatalysts by IMP, PD and DP methods was the same as that of unmodified TiO_2.

The Au loading by these three methods did not change the value of the main band gap as compared to the unmodified TiO_2 (see Table 2). However, the presence of Au particles on the TiO_2 surface contributed to the increase in the visible-light-harvesting ability ($\lambda > 400$ nm). The graphs (Figure 5a) show that Au particles on the TiO_2 surface significantly enhanced the visible light-harvesting ability up to a wavelength of 800 nm. The PL emission spectra of all Au-loaded TiO_2 and the unmodified TiO_2 were analyzed and shown in Figure 5b. All Au-loaded TiO_2 provided lower spectra intensities than that of the unmodified TiO_2. This pointed out that the existence of Au particles on the TiO_2 surface could be an electron trapping site leading to a reduction in the recombination rate between the photo generated electrons and photo generated holes (Bamwenda et al., 1995).

Figure 5b also shows the effect of the Au loading method on the electron trapping efficiency of the Au particles on the TiO_2 surface. The DP method may result in some Au particles being located within the bulk of the TiO_2 network. These bulk Au sites had a higher affinity for capturing and retaining excited electrons compared to surface Au sites, leading to a reduced recombination rate between electrons and holes. Consequently, TiO_2 loaded with Au using the DP method exhibited the lowest PL emission intensity.

3.3 Photocatalytic H_2 production: Effects of synthesis methods

The photocatalytic activities of Au-loaded TiO_2 synthesized by SG, ST and FSP methods as compared to the commercial TiO_2 (P25) were examined by using the photocatalytic H_2 production rate as an indicator via the formic acid photodegradation reaction under simulated sunlight. As shown in Figure 6, the 0.26 % w/w Au-loaded TiO_2 synthesized by the ST method exhibited the highest photocatalytic activity. It provided the H_2 production rate of~6,000 $\mu mol_{H2}/h/g_{cat}$.

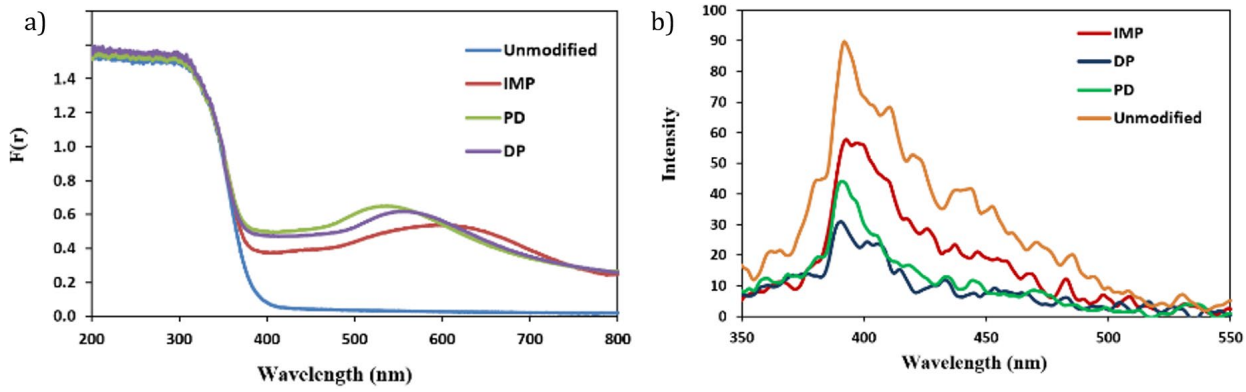

Figure 5. a) UV-vis: DRS results of Au-loaded TiO_2 by IMP, PD, and DP methods; b) The PL emission spectra of Au-loaded TiO_2 by IMP, PD, and DP methods

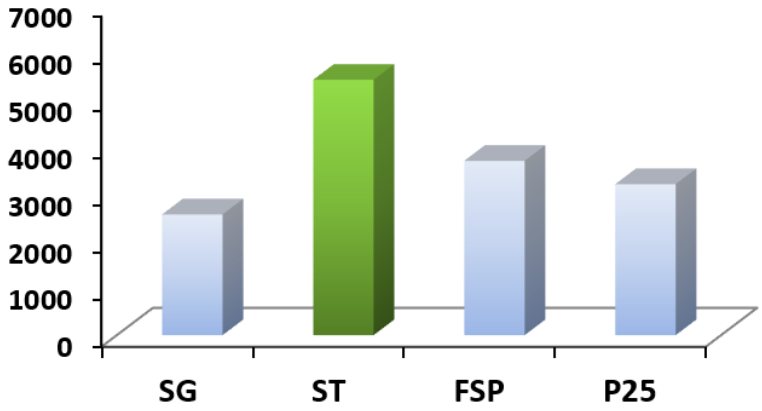

Figure 6. H_2 production of the 0.26 % w/w Au-loaded TiO_2 by PD method photocatalysts under simulated sunlight**:** Effects of synthesis methods on the photocatalytic activity

This is probably because the ST method provided the synthesized TiO_2 with the high specific surface area (compared to the SG-synthesized TiO_2) and the small nano-crystallite size with agglomeration structure (compared to the FSP-synthesized TiO_2). The high surface area and the agglomeration structure contributed to the high active sites that are exposed to the liquid phase and the high amount of onset excited electrons at one point, respectively, resulting in the high photocatalytic activity. In addition**,** the ST method provided the TiO_2 with a suitable pore size in the mesoporous range. The mesopore size enhanced the surface access of the liquid species reactant, leading to the increase in the photocatalytic activity of TiO_2. Thereby ST method was selected to further find out the suitable condition of preparation to get the higher efficient TiO_2 photocatalyst.

3.4 Photocatalytic H_2 production: Effects of Au loading methods

The photocatalytic H_2 production rates of all Au-loaded TiO_2 as compared to the unmodified TiO_2 shown in Figure 7 exhibited the effect of the existence of Au particles on the TiO_2 surface and the loading methods on the photocatalytic activity of TiO_2-based photocatalyst. The result showed that the existence of Au particles on the TiO_2 surface significantly enhanced the photocatalytic activity of the unmodified TiO_2. The roles of Au particles as the electron trapping and coactive site contribute to the proton reduction reaction, leading to the increase in the H_2 production rates (Bamwenda et al., 1995). The Au-loaded TiO_2 by the DP and PD methods showed higher photocatalytic activity than that of the Au-loaded TiO_2 by the IMP method. Both the DP and PD methods resulted in higher Au dispersion compared to the IMP method (Table 2). This increased dispersion led to a higher number of Au coactive sites. The photocatalytic activity of Au-loaded TiO_2 prepared by DP and PD methods was similar; this probably due to a synergistic effect between the dispersion of Au particles and their recombination suppression properties. While the Au dispersion of Au-loaded TiO_2 prepared by the DP method was lower than that of Au-loaded TiO_2 prepared by the PD method (Table 2), the DP method exhibited a superior recombination retardance ability (Figure 5b). This balance between dispersion and recombination properties led to comparable photocatalytic activities for both DP and PD-prepared catalysts.

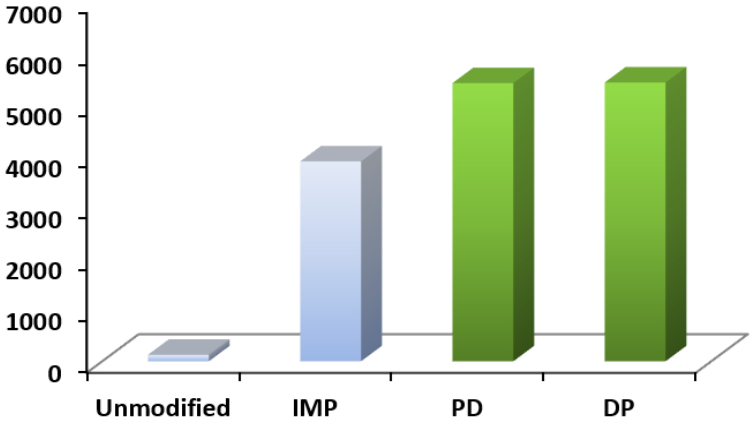

Figure 7. H_2 production of the 0.26 % w/w Au-loaded TiO_2 (synthesized by the ST method) under simulated sunlight: Effect of Au loading method on photocatalytic activity

4. CONCLUSION

The solvothermal method was successfully employed to synthesize TiO_2 photocatalyst particles with a mesoporous-agglomerated structure and a small nano-crystallite size. These characteristics, combined with the high specific surface area provided by the ST method, contributed to the enhanced photocatalytic activity. The Au coactive sites introduced using PD and DP methods demonstrated a superior ability to suppress charge recombination compared to those loaded by IMD.

ACKNOWLEDGMENTS

This work was supported by Silpakorn University Research, Innovation and Creative Fund and Department of Chemical Engineering, Faculty of Engineering and Industrial Technology, Silpakorn University, Thailand.

REFERENCES

Abdelli, H., Hamoud, H. I., Bolletta, J. P., Paecklar, A., Bardaoui, A., Kostov, K. L., Szaniawska, E., Maignan, A., Martin, C., & El-Roz, M. (2023). H_2 production from formic acid over highly stable and efficient Cu-Fe-O spinel based photocatalysts under flow, visible-light and at room temperature conditions. *Applied Materials Today*, *31*, Article 101771. https://doi.org/10.1016/j.apmt.2023.101771

Ahmad, K., Ghatak, H. R., & Ahuja, S. M. (2020). A review on photocatalytic remediation of environmental pollutants and H_2 production through water splitting: A sustainable approach. *Environmental Technology & Innovation*, *19*, Article 100893. https://doi.org/10.1016/j.eti.2020.100893

Araña, J., Cabo, C. G., Dona-Rodrıguez, J. M., González-Dıaz, O., Herrera-Melián, J. A., & Pérez-Peña, J. (2004). FTIR study of formic acid interaction with TiO_2 and TiO_2 doped with Pd and Cu in photocatalytic processes. *Applied Surface Science*, *239*(1), 60–71. https://doi.org/10.1016/j.apsusc.2004.04.039

Bamwenda, G. R., Tsubota, S., Nakamura, T., & Haruta, M. (1995). Photoassisted hydrogen production from a water-ethanol solution: A comparison of activities of Au-TiO_2 and Pt-TiO_2. *Journal of Photochemistry and Photobiology A: Chemistry*, *89*(2), 177–189. https://doi.org/10.1016/1010-6030(95)04039-I

Bhuskute, B. D., Ali-Löytty, H., Honkanen, M., Salminen, T., & Valden, M. (2022). Influence of the photodeposition sequence on the photocatalytic activity of plasmonic Ag–Au/TiO_2 nanocomposites. *Nanoscale Advances*, *4*(20), 4335–4343. https://doi.org/10.1039/d2na00440b

Boningari, T., Inturi, S. N. R., Suidan, M., & Smirniotis, P. G. (2018). Novel one-step synthesis of sulfur doped-TiO_2 by flame spray pyrolysis for visible light photocatalytic degradation of acetaldehyde. *Chemical Engineering Journal*, *339*, 249–258. https://doi.org/10.1016/j.cej.2018.01.063

Bouhadoun, S., Guillard, C., Dappozze, F., Singh, S., Amans, D., Bouclé, J., & Herlin-Boime, N. (2015). One step synthesis of N-doped and Au-loaded TiO_2 nanoparticles by laser pyrolysis: Application in photocatalysis. *Applied Catalysis B: Environment and Energy*, *174–175*, 367–375. https://doi.org/10.1016/j.apcatb.2015.03.022

Cao, D., Wang, Q., Wu, Y., Zhu, S., Jia, Y., & Wang, R. (2020). Solvothermal synthesis and enhanced photocatalytic hydrogen production of Bi/Bi_2MoO_6 co-sensitized TiO_2 nanotube arrays. *Separation and Purification Technology*, *250*, Article 117132. https://doi.org/10.1016/j.seppur.2020.117132

Chan, S. C., & Barteau, M. A. (2005). Preparation of highly uniform Ag/TiO_2 and Au/TiO_2 supported nanoparticle catalysis by photodeposition. *Langmuir*, *21*(12), 5588–5595. https://doi.org/10.1021/la046887k

Chiarello, G. L., Aguirre, M. H., & Selli, E. (2010). Hydrogen production by photocatalytic steam reforming of methanol on noble metal-modified TiO_2. *Journal of Catalysis*, *273*(2), 182–190. https://doi.org/10.1016/j.jcat.2010.05.012

Chiarello, G. L., Selli, E., & Forni, L. (2008). Photocatalytic hydrogen production over flame spray pyrolysis-synthesised TiO_2 and Au/TiO_2. *Applied Catalysis B: Environmental*, *84*(1–2), 332–339. https://doi.org/10.1016/j.apcatb.2008.04.012

Chung, K.-H., Park, Y.-K., Kim, S.-J., Kim, S.-C., & Jung, S.-C. (2023). Green hydrogen production from ammonia water by liquid–plasma cracking on solid acid catalysts. *Renewable Energy*, *216*, Article 119052. https://doi.org/10.1016/j.renene.2023.119052

Farias, J., Albizzati, E. D., & Alfano, O. M. (2009). Kinetic study of the photo-Fenton degradation of formic acid: Combined effects of temperature and iron concentration. *Catalysis Today*, *144*(1–2), 117–123. https://doi.org/10.1016/j.cattod.2008.12.027

Gonzalez, V. R., Zanella, R., Angel, G. D., & Gomez, R. (2008). MTBE visible-light photocatalytic decomposition over Au/TiO_2 and Au/TiO_2-Al_2O_3 sol-gel prepared catalysts. *Journal of Molecular Catalysis A: Chemical*, *281*(1–2), 93–98. https://doi.org/10.1016/j.molcata.2007.07.009

Guo, W., Guo, T., Zhang, Y., Yin, L., & Dai, Y. (2023). Progress on simultaneous photocatalytic degradation of pollutants and production of clean energy: A review. *Chemosphere*, *339*, Article 139486. https://doi.org/10.1016/j.chemosphere.2023.139486

Gupta, A., Likozar, B., Jana, R., Chanu, W. C., & Singh, M. K. (2022). A review of hydrogen production processes by photocatalytic water splitting–From atomistic catalysis design to optimal reactor engineering. *International Journal of Hydrogen Energy*, *47*(78), 33282–33307. https://doi.org/10.1016/j.ijhydene.2022.07.210

Guzmán, C., Del Angel, G., Gómez, R., Galindo, F., Zanella, R., Torres, G., Angeles-Chavez, C., & Fierro, J. L. G. (2009). Gold particle size determination on Au/TiO_2-CeO_2 catalysts by means of carbon monoxide, hydrogen chemisorption and transmission electron microscopy. *Journal of Nano Research*, *5*, 13–23. https://doi.org/10.4028/www.scientific.net/JNanoR.5.13

Hayat, A., Ali, H., Ajmal, Z., Alshammari, A., Alghamdi, M. M., El-Zahhar, A. A., Almuqati, N., Sohail, M., Abu-Dief, A. M., Khan, S., Al-Hadeethi, Y., Ansari, M. Z., & Orooji, Y. (2024). Emerging breakthroughs in covalent triazine frameworks: From fundamentals towards photocatalytic water splitting and challenges. *Progress in Materials Science*, *147*, Article 101352. https://doi.org/10.1016/j.pmatsci.2024.101352

Hidalgo, M. C., Maicu, M., Navío, J. A., & Colón, G. (2009). Effect of sulfate pretreatment on gold-modified TiO_2 for photocatalytic applications. *The Journal of Physical Chemistry C*, *113*(29), 12840–12847. https://doi.org/10.1021/jp903432p

Huang, B. S., & Wey, M. Y. (2011). Properties and H_2 production ability of Pt photodeposited on the anatase phase transition of nitrogen-doped titanium dioxide. *International Journal of Hydrogen Energy*, *36*(16), 9479–9486. https://doi.org/10.1016/j.ijhydene.2011.05.064

Kang, M. (2003). Synthesis of Fe/TiO_2 photocatalyst with nanometer size by solvothermal method and the effect of H_2O addition on structural stability and photodecomposition of methanol. *Journal of Molecular Catalysis A: Chemical*, *197*(1–2), 173–183. https://doi.org/10.1016/S1381-1169(02)00586-1

Kang, M., Ko, Y. R., Jeon, M. K., Lee, S. C., Choung, S. J., Park, J. Y., Kim, S., & Choi, S. H. (2005). Characterization of Bi/TiO_2 nanometer size particle synthesized by solvothermal method and CH_3CHO decomposition in a plasma-photocatalytic system. *Journal of Photochemistry and Photobiology A: Chemistry*, *173*(2), 128–136. https://doi.org/10.1016/j.jphotochem.2004.12.030

Kang, M., Lee, S. Y., Chung, C. H., Cho, S. M., Han, G. Y., Kim, B. W., & Yoon, K. J. (2001). Characterization of a $TiO2$ photocatalyst synthesized by the solthermal method and its catalytic performance for $CHCl_3$ decomposition. *Journal of Photochemistry and Photobiology A: Chemistry*, *144*(2–3), 185–191. https://doi.org/10.1016/S1010-6030(01)00501-9

Khan, M. A., Woo, S. I., & Yang, O. B. (2008). Hydrothemally stabilized Fe(III) doped titania active under visible light for water splitting reaction. *International Journal of Hydrogen Energy*, *33*(20). 5345–5351. https://doi.org/10.1016/j.ijhydene.2008.07.119

Khtaee, A. R., & Kasiri, M. B. (2010). Photocatalytic degradation of organic dyes in the presence of nanostructured titanium dioxide: Influence of the chemical structure of dyes. *Journal of Molecular Catalysis A: Chemical*, 328(1–2), 8–26. https://doi.org/10.1016/j.molcata.2010.05.023

Kongsuebchart, W., Prasertdam, P., Panpranot, J., Sirisuk, A., Supphasrirongjaroen, P., & Satayaprasert, C. (2006). Effect of crystallite sie on the surface defect of nano-TiO_2 prepared via solvothermal synthesis. *Journal of Crystal Growth*, *297*(1), 234–238. https://doi.org/10.1016/j.jcrysgro.2006.09.018

Lee, Y., Chae, J., & Kang, M. (2010). Comparison of the photovoltaic efficiency on DSSC for nanometer sized TiO_2 using a conventional sol-gel and solvothermal methods. *Journal of Industrial and Engineering Chemistry*, *16*(4), 609–614. https://doi.org/10.1016/j.jiec.2010.03.008

Lin, X., Rong, F., Fu, D., & Yuan, C. (2012). Enhanced photocatalytic activity of fluorine doped TiO_2 by loaded with Ag for degradation of organic pollutants. *Powder Techno*, *219*, 173–178. https://doi.org/10.1016/j.powtec.2011.12.037

Liu, G., Wang, L., Yang, H. G., Cheng, H. M., & Lu, G. Q. (2010). Titania-based photocatalysts—crystal growth, doping and heterostructuring. *Journal of Materials Chemistry*, *20*(5), 831–843. https://doi.org/10.1039/B909930A

Mahdavi-Shakib, A., Sravan-Kumar, K. B., Whittaker N. T., Xie, T., Grabow, C. L., Rioux, M. R., & Chandler, D. B. (2021). Kinetics of H_2 adsorption at the metal–support interface of Au/TiO_2 catalysts probed by broad background IR absorbance. *Angewandte Chemie International Edition*, *60*(14), 7735–7743. https://doi.org/10.1002/anie.202013359

Meyer, R., Lemire, C., Shaikhutdinov, Sh. K., & Freund, H.-J. (2004). Surface chemistry of catalysis by gold. *Gold Bulletin*, *37*(1–2), 72–124. https://doi.org/10.1007/BF03215519

Mueller, R., Madler, L., & Pratsinis, S. E. (2003). Nanoparticle synthesis at high production rates by flame spray pyrolysis. *Chemical Engineering Science*, *58*(10), 1969–1976. https://doi.org/10.1016/S0009-2509(03)00022-8

Nam, W. S., & Han, G. Y. (2003). Characterization and photocatalytic performance of nanosize TiO_2 powders prepared by the solvothermal method. *Korean Journal of Chemical Engineering*, *20*(6), 1149–1153. https://doi.org/10.1007/BF02706953

Osterloh, F. E., & Parkinson, B. A. (2011). Recent developments in solar water-splitting photocatalysis. *MRS Bulletin*, *36*(1), 17–22. https://doi.org/10.1557/mrs.2010.5

Patsoura, A., Kondarides, D. I., & Verykios, X. E. (2007). Photocatalytic degradation of organic pollutants with simultaneous production of hydrogen. *Catalysis Today*, *124*(3–4), 94–102. https://doi.org/10.1016/j.cattod.2007.03.028

Pawinrat, P., Mekasuwandumrong, O., & Panpranot, J. (2009). Synthesis of Au-ZnO and Pt-ZnO nanocomposites by one-step flame spray pyrolysis and its application for photocatalytic degradation of dyes. *Catalysis Communications*, *10*(10), 1380–1385. https://doi.org/10.1016/j.catcom.2009.03.002

Payakgul, W., Mekasuwandumrong, O., Pavarajarn, V., & Praserthdam, P. (2005). Effects of reaction medium on the synthesis of TiO_2 nanocrystals by thermal decomposition of titanium (IV) n-butoxide. *Ceramics International*, *31*(3), 391–397. https://doi.org/10.1016/j.ceramint.2004.05.025

Peng, T., Ke, D., Cai, P., Daia, K., Ma, L., & Zan, L. (2008). Influence of different ruthenium (II) bipyridyl complex on the photocatalytic H_2 evolution over TiO_2 nanoparticles with mesostructures. *Journal of Power Sources*, *180*(1), 498–505. https://doi.org/10.1016/j.jpowsour.2008.02.002

Puangpetch, T., Chavadej, S., & Sreethawong, T. (2011). Hydrogen production over Au-loaded mesoporous-assembled $SrTiO_3$ nanocrytal photocatalyst: Effects of molecular structure and chemical properties of hole scavengers. *Energy Convers Manage*, *52*(5), 2256–2261. https://doi.org/10.1016/j.enconman.2010.12.026

Puangpetch, T., Sreethawong, T., & Chavadej, S. (2010). Hydrogen production over metal-loaded mesoporous-assembled $SrTiO_3$ nanocrystal photocatalysis: Effects of metal type and loading. *International Journal of Hydrogen Energy*, *35*(13), 6531–6540. https://doi.org/10.1016/j.ijhydene.2010.04.015

Puangpetch, T., Sreethawong, T., Yoshikawa, S., & Chavadej, S. (2008). Synthesis and photocatalytic activity in methyl orange degradation of mesoporous-assembled $SrTiO_3$ nanocrystals prepared by sol–gel method with the aid of structure-directing surfactant. *Journal of Molecular Catalysis A: Chemical*, *287*(1–2), 70–79. https://doi.org/10.1016/j.molcata.2008.02.027

Puangpetch, T., Sreethawong, T., Yoshikawa, S., & Chavadej, S. (2009). Hydrogen production from photocatalytic water splitting over mesoporous-assembled $SrTiO_3$ nanocrystal-based photocatalysts. *Journal of Molecular Catalysis A: Chemical*, *312*(1–2), 97–106. https://doi.org/10.1016/j.molcata.2009.07.012

Rodríguez-Martínez, C., García-Domínguez, Á. E., Guerrero-Robles, F., Saavedra-Díaz, R. O., Torres-Torres, G., Felipe, C., Ojeda-López, R., Silahua-Pavón, A., & Cervantes-Uribe, A. (2020). Synthesis of supported metal nanoparticles (Au/TiO_2) by the suspension impregnation method. *Journal of Composites Science*, *4*(3), Article 89. https://doi.org/10.3390/jcs4030089

Rouquerol, F., Rouquerol, J., & Sing, K. (1999). *Adsorption by powders and porous solids: Principles, methodology and applications*. Academic Press.

Rusinque, B., Escobedo, S., & de Lasa, H. (2019). Photocatalytic hydrogen production under near-UV using Pd-doped mesoporous TiO_2 and ethanol as organic scavenger. *Catalysts*, *9*(1), Article 33. https://doi.org/10.3390/catal9010033

Sadek, O., Touhtouh, S., Dahbi, A., & Hajjaji, A. (2023). Photocatalytic degradation of methylene blue on multilayer TiO_2 coatings elaborated by the sol-gel spin-coating method. *Water, Air, & Soil Pollution*, *234*, Article 698. https://doi.org/10.1007/s11270-023-06558-4

Sasikala, R., Sudarsan, V., Sudakar, C., Naik, R., Panicker, L., & Bharadwaj, S. R. (2009). Modification of the photocatalytic properties of self doped TiO_2 nanoparticles for hydrogen generation using sunlight type radiation. *International Journal of Hydrogen Energy*, *34*(15), 6105–6113. https://doi.org/10.1016/j.ijhydene.2009.05.131

Solanki, K., Parmar, D., Savaliya, C., Kumar, S., & Jethva, S. (2022). Surface morphology and optical properties of sol-gel synthesized TiO_2 nanoparticles: Effect of Co, Pd and Ni-doping. *Materials Today: Proceedings*, *50*(Part 6), 2576–2580. https://doi.org/10.1016/j.matpr.2021.10.182

Sreethawong, T., Junbua, C., & Chavadej, S. (2009a). Photocatalytic H_2production from water splitting under visible light light irradiation using eosin Y-sensitized mesoporous-assembled Pt/TiO_2 nanocrystal photocatalyst. *Journal of Power Sources*, *190*(2), 513–524. https://doi.org/10.1016/j.jpowsour.2009.01.054

Sreethawong, T., Laehsalee, S., & Chavadej, S. (2008). Comparative investigation of mesoporous- and non-mesoporous-assembled TiO_2 nanocrystals for photocatalytic H_2 production over N-doped TiO_2 under visible light irradiation. *International Journal of Hydrogen Energy*, *33*(21), 5947–5957. https://doi.org/10.1016/j.ijhydene.2008.08.007

Sreethawong, T., Laehsalee, S., & Chavadej, S. (2009b). Use of Pt/N-doped mesoporous-assembled nanocrystalline TiO_2 for photocatalytic H_2 production under visible light irradiation. *Catalysis Communications*, *10*(5), 538–543. https://doi.org/10.1016/j.catcom.2008.10.029

Strobel, R., Baiker, A., & Pratsinis, S. E. (2006). Flame aerosol synthesis of smart catalysts. *Advanced Powder Technology*, *17*(5), 457–480. https://doi.org/10.1163/156855206778440525

Strobel, R., & Pratsinis, S. E. (2007). Flame aerosol synthesis of smart nanostructured materials. *Journal of Materials Chemistry*, *17*(45), 4743–4756. https://doi.org/10.1039/B711652G

Teoh, W. Y., Amal, R., & Madler, L. (2010). Flame spray pyrolysis: An enabling technology for nanoparticles design and fabrication. *Nanoscale*, *2*(8), 1324–1347. https://doi.org/10.1039/C0NR00017E

Teoh, W. Y., Madler, L., Beydoun, D., Pratsinis, S. E., & Amal, R. (2005). Direct (one-step) synthesis of TiO_2 and Pt/TiO_2 nanoparticles for photocatalytic mineralization of sucrose. *Chemical Engineering Science*, *60*(21), 5852–5861. https://doi.org/10.1016/j.ces.2005.05.037

Wang, Q., Ren, C., Zhao, Y., Fang, F., Yin, Y., Ye, Y., Yang, K., Yang, Q., & Wang, K. (2023a). Photocatalytic pollutant elimination and hydrogen production over TiO_2 NTs/Bi2S_3-MoS_2 with Z-scheme configuration: Kinetics and mechanism. *Materials Research Bulletin*, *167*, Article 112430. https://doi.org/10.1016/j.materresbull.2023.112430

Wang, Q., Zhao, Y., Zhang, Z., Liao, S., Deng, Y., Wang, X., Ye, Q., & Wang, K. (2023b). Hydrothermal preparation of Sn_3O_4/TiO_2 nanotube arrays as effective photocatalysts for boosting photocatalytic dye degradation and hydrogen production. *Ceramics International*, *49*(4), 5977–5985. https://doi.org/10.1016/j.ceramint.2022.11.113

Wang, S., Shiraishi, F., & Nakano, K. (2002). A synergistic effect of photocatalysis and ozonation on decomposition of formic acid in an aqueous solution. *Chemical Engineering Journal*, *87*(2), 261–271. https://doi.org/10.1016/S1385-8947(02)00016-5

Yan, H., & Yang, H. (2011). TiO_2-g-C_3N_4 composite materials for photocatalytic H_2 evolution under visible light irradiation. *Journal of Alloys and Compounds*, *509*(4), L26–L29. https://doi.org/10.1016/j.jallcom.2010.09.201

Yan, Z., Yin, K., Xu, M., Fang, N., Yu, W., Chu, Y., & Shu, S. (2023). Photocatalysis for synergistic water remediation and H_2 production: A review. *Chemical Engineering Journal*, *472*, Article 145066. https://doi.org/10.1016/j.cej.2023.145066

Zhang, Y. J., & Zhang, L. (2009). Photocatalytic degradation of formic acid with simultaneous production of hydrogen over Pt and Ru-loaded CdS/Al-HMS photocatalysts. *Desalination*, *249*(3), 1017–1021. https://doi.org/10.1016/j.desal.2009.09.011